JOURNAL OF MATERIALS SCIENCE 33 (1998) 2857–2868

Structure development in PET/PA6 microfibrillar-reinforced composites as revealed by microhardness

M. KRUMOVA, S. FAKIROV*, F. J. BALTÁ CALLEJA
Instituto de Estructura de la Materia, CSIC, 28006 Madrid, Spain
E-mail: embalta@icm.csic.cs
M. EVSTATIEV
Laboratory on Structure and Properties of Polymers, University of Sofia, 1126 Sofia, Bulgaria

Homopolymer poly(ethylene terephthalate) (PET) and nylon-6 (PA6) and a blend (1:1 by weight) of these polymers, were extruded as strips and ultraquenched from the melt. After zone drawing and additional annealing at temperatures, T_a, of 220 or 240 °C for 5 or 25 h in vacuum, the samples were studied by scanning electron microscopy (SEM), wide-angle X-ray scattering, solubility and microhardness, H, tests. In conformity with previous studies of the same system, the present SEM observations show that mechanical drawing results in the formation of a highly oriented fibrillar structure of PET which is preserved even after annealing above the melting point of PA6. Furthermore, raising of both annealing temperature and duration up to 240 °C and 25 h, respectively, results in a strong decrease of the solubility of the PA6 fraction in formic acid (five-fold). This is attributed to intensive chemical interactions between components, drastically improving the adhesion between matrix and reinforcing microfibrils. From the dependence of H on degree of crystallinity, w_c, the hardness values for completely amorphous, H_a, and fully crystalline, H_c, neat homopolymers were extrapolated ($H_a^{PET}=128$ MPa, $H_c^{PET}=294$ MPa, $H_a^{PA}=52$ MPa and $H_c^{PA}=283$ MPa). Using these values and applying the additive law, the H-value of the microfibrils is derived. The high value obtained for PET fibrils (360 MPa) is explained by the peculiarity in the structure formation of these microfibrils. The effect of crystal size on the formation of H is also discussed. The H-value of infinite large PA6 crystals is derived to be $H^{\infty}=460$ MPa. It is shown that the type and extent of the mutual dispersion of the components, as well as the adhesion between them, are important factors for the proper applicability of the additive law. © *1998 Kluwer Academic Publishers*

1. Introduction

The commercial importance of polymer blends and polymer composites is significant – only polymer blends constitute currently over 30% of the polymer market [1]. In addition, polymer blending is of great interest to researchers as it represents an approach to the achievement of new combinations of defined properties without having to synthesize novel chain structures. However, blending of two polymers usually results in immiscibility and a third component, i.e. a compatibilizer such as a block copolymer, has to be added. A similar problem also exists in the case of fibre-reinforced composites where, in addition to the length-to-diameter ratio, i.e. the aspect ratio, good adhesion between the fibre and the surrounding matrix is required and coupling agents coating the fibres are used.

A new type of polymer composites satisfying to a great extent the outlined peculiarities of polymer blends and composites was recently developed [2–9]. Unlike the classical macrocomposites (e.g. fibre-reinforced ones) and the molecular composites (with "single" rod-like macromolecules as reinforcing elements), a third group of polymer composites which is reinforced by microfibrils has been introduced as microfibrillar-reinforced composites (MFC) [2].

Macrocomposites and their "molecular" analogues are prepared in the same way – by blending the matrix material with the reinforcing material usually through melting. This approach is not applicable to MFCs because microfibrils are not available as a separate material. The fibrils are created during MFC production by drawing the polymer blend, leading to the orientation of both components (fibrillization)

* *Permanent address*: Laboratory on Structure and Properties of Polymers, University of Sofia, 1126 Sofia, Bulgaria.

followed by melting of the lower melting component (isotropization) with preservation of the oriented microfibrillar structure of the higher melting component [2–9].

It is important to note that, in addition to isotropization during short (several hours) thermal treatment, chemical reactions (additional condensation and transreactions) between condensation polymers in the melt [10], as well as in the bulk solid state [11], take place at the interfaces, resulting in the formation of a copolymeric interphase. The latter plays the role of a compatibilizer, i.e. one deals with a self-compatibilization effect as far as there is no need to introduce to the blend an extra synthesized copolymer of the blend components according to the usual approach [12–14].

Finally, it should be mentioned that this new type of composite (MFC) exhibits mechanical properties (Young's modulus and tensile strength) which are higher by 30%–50% than the weight average values of the independent components and comparable to those of glass fibre-reinforced composites having the same matrix, thus confirming their composite nature [3–9].

Hardness, H, has been shown to be a promising technique for the microstructural investigation of multicomponent blends and can provide information on the degree of interpenetration of the blend components [15]. The case of blends of low- and high-density polyethylene (PE) is an example where hardness can be described in terms of an additive system of two independent components [16]. However, in systems like polyethylene/polypropylene blends prepared from semidilute solution or poly(butylene terephthalate) (PBT)/polycarbonate blends, a deviation from the additivity law is detected [17, 18]. In these cases the deviation of H from the additive behaviour of the single components can be related to the changes of crystallinity and thickness of the crystals. It is worth mentioning that in the case of blends of condensation polymers, in contrast to polyolefines, the blend partners can interact chemically and form copolymers. For this reason the observed deviation from the additivity law for such systems can be also related to the chemical changes taking place during blending. In order to distinguish between the contribution of crystallinity factors and chemical changes one has to investigate condensation blends in the glassy state.

In a very recent study [19], the microhardness of coreactive blends of PET and bisphenol A polycarbonate (PC) was investigated over the whole range of compositions. The occurrence of one single glass transition temperature, T_g, step in the DSC curves indicated that intensive chemical interactions had taken place during melt blending, resulting in the formation of copolycondensates with dominating random sequential order. The parallel decrease of microhardness and of glass transition temperature with increasing PET content in the blends has been ascribed to the formation of new copolymer molecules enriched in the component characterized by lower H and T_g values.

The aims of the present work were as follows: (i) to supplement our earlier studies on MFC of condensation polymers, where evidence for chemical interactions was observed [3–9] with reference to the microhardness additivity of the two components. We have focused our attention on the structure formation of MFC during their manufacture as revealed by microhardness; (ii) to examine the relationship between the microhardness of MFC and that of the constituting components including the morphological entities. For this reason the two neat partners of MFC were subjected to the same thermal and mechanical treatments and characterized after each step as the MFC; (iii) to evaluate the microhardness of the reinforcing microfibrils upon application of the additive law and to discuss the effect of the crystal size on the structure formation.

2. Experimental procedure

2.1. Materials

The polymers used were PET (Goodyear Merge 1934F, $M_n = 23\,400$) and PA6 (Allied Signal Capron 8200), $M_n = 20\,600$). These polymers were ground to a particle size of less than 0.4 mm (after cooling in liquid nitrogen) and then mixed in the solid state (1 : 1 wt/wt). Films of this blend and of the respective homopolymers were prepared according to the following procedure. A capillary rheometer, flushed with argon and heated to about 280 °C, was loaded with powdered material. The melt obtained was kept in the rheometer for 5–6 min and then extruded through the capillary (1 mm diameter) on metal rolls rotating at about 30 rev min^{-1}. The rolls were immersed in a quenching bath of liquid nitrogen. Films of both homopolymers and the blend with different thicknesses (0.10–0.13 mm) and widths (4–5 mm) were prepared by varying the extrusion rate and distance between the rolls.

2.2. Techniques

2.2.1. Differential scanning calorimetry

It was established by X-ray and calorimetric studies that, immediately after quenching, PET was completely amorphous while the films of PA6 and the PET/PA6 blend (designated as sample B) were partially crystalline.

All films were oriented according to the method of zone drawing [20, 21] under the following conditions: the zone drawing was performed on the as-quenched films by moving a specially designed heater (a narrow cylindrical element, diameter 2 mm), attached to the crosshead of a Zwick tensile testing machine, from the lower to the upper part of the samples under tension. The heater was moved at 10 mm min^{-1}. A tension of 15 MPa was applied to the films. The temperature of the heater was 85 ° C for PET and 180 ° C for PA6 and the PET/PA6 blend. The zone-drawn films were subsequently annealed in vacuum with fixed ends at 220 or 240 °C for 5 or 25 h. The sample preparation conditions are given in Table I.

The degree of crystallinity has been determined [3] from calorimetric data, w_c (DSC), according to the

TABLE I Preparation conditions of microfibrillar-reinforced composites

Sample designation	Composition PA/PET (wt %)	Zone drawing		Annealing in vacuum with fixed ends	
		Temperature[a] (°C)	Draw ratio (λ)	T_a (°C)	t_a (*h*)
PET-Q (quenched)	0/100	–	–	–	–
PET-D	0/100	85	4.0	–	–
PET-D-1	0/100	85	4.0	220	5
PET-D-2	0/100	85	4.0	220	25
PET-D-4	0/100	85	4.0	240	25
PA-Q (quenched)	100/0	–	–	–	–
PA-D	100/0	180	3.8	–	–
PA-D-1	100/0	180	3.8	220	5
PA-D-2	100/0	180	3.8	220	25
B-Q (quenched)	50/50	–	–	–	–
B-D	50/50	180	4.2	–	–
B-D-1	50/50	180	4.2	220	5
B-D-2	50/50	180	4.2	220	25
B-D-3	50/50	180	4.2	240	5
B-D-4	50/50	180	4.2	240	25

[a] All samples were annealed at the moving speed of the heater, 10 mm min^{-1}; tension applied, 15 MPa.

equation

$$w_c = \frac{(\Delta H_f - \Delta H_c)}{F\Delta H^\circ} \quad (1)$$

where ΔH_f and ΔH_c are the values of heat of fusion and of cold crystallization, respectively, during the same heating run, F is the weight fraction of the homopolymers in the blend (in the present case 0.5) and $\Delta H^\circ = 230$ kJ kg^{-1} and $\Delta H^\circ = 140$ kJ kg^{-1} are the ideal values of the heat of melting for PA6 [22] and PET [23], respectively.

2.2.2. X-ray scattering

Wide-angle X-ray scattering (WAXS) patterns as well as equatorial and meridional diffractograms were obtained for all drawn and annealed blends using a Siemens diffractometer with nickel-filtered CuK_α radiation. 2θ scans from 10°–40° were made. The size of the coherently diffracting domains (crystallite size) of the samples was directly calculated from the integral breadth δβ according to $\delta\beta \sim 1/D_{hkl}$ [24]. This obviously provides a minimum value for the crystallite size. The lateral crystallite size for PA6 was determined from the (2 0 0) reflection and for PET from the equatorial scan of the (0 1 0) reflection. The size of the PET crystallites in the axial direction was assessed from the meridional scan of the ($\bar{1}$ 0 5) reflection.

The X-ray data were also used to estimate the degree of crystallinity [3]. To determine the relative crystallinity, w_c (WAXS), a standard procedure was used, according to which the amorphous peak (the shape of which is determined by the WAXS pattern of as-quenched PET) is fitted to the diffraction curve so that it intersects at some points near its maximum with crystalline minima; the area under the amorphous curve is subtracted from the total diffraction pattern to yield I_c, the portion of the diffraction attributable to the crystalline regions. w_c (WAXS) is then the ratio of the integrated area under the crystalline peaks to the total integrated area, I_t, under the WAXS scan ($\Sigma I_c/\Sigma I_t$). No attempt was made to separate PET and PA6 independent amorphous contributions.

Using a Kratky camera, small-angle X-ray scattering (SAXS) curves of the homopolymers and blends with different thermal prehistory were recorded, from which the long spacing, L, was estimated [3].

2.2.3. Microscopy

A Jeol JSM 5400 scanning electron microscope (SEM) with an accelerating voltage of 25 kV was used for the observation of the samples. Specimens were prepared by peeling along the length of the drawn blends or by preparing a fracture surface after cooling in liquid nitrogen. Specimens for observation of the microfibrils were prepared from the drawn blends by extraction of PA6 with formic acid for 24 h. All specimens were mounted and coated with gold before analysis.

2.2.4. Mechanical studies

Mechanical tests were carried out at room temperature, at a crosshead speed of 5 mm min^{-1}, using a Zwick 1464 tensile tester equipped with an incremental extensiometer [3]. Young's modulus (E, in the deformation range from 0.05%–0.5%) and tensile strength, σ, were determined from the load–extension curves, as was the relative deformation at break, ε_b. All values are averaged from five measurements.

Microhardness, H, was measured at room temperature using a Leitz Tester equipped with a square-based diamond indentor. The H-value was derived from the residual projected area of indentation according to the expression

$$H = \frac{kP}{d^2} \text{ (Pa)} \quad (2)$$

where d is the length (m) of the impression diagonal P, the contact load applied (N), and k is a geometrical factor equal to 1.854. A loading cycle of 0.1 min and loads of 49, 98, 147 and 245 mN were used. Ten measurements for each data point were averaged.

It is known [25] that for oriented materials an anisotropic shape of the indentation appears. A higher H value is derived from the indentation diagonal parallel to the fibre axis. The low H value is calculated from the diagonal perpendicular to it. The first one corresponds to the instant elastic recovery in the draw direction, the second one to the plastic deformation of the oriented material. In the present study, only the values of H in the direction perpendicular to the orientation axis will be discussed and further designated as H.

Finally, for comparative and other purposes, the microhardness was evaluated by means of the additive law

$$H = \sum_{i=1}^{\infty} H_i \varphi_i \tag{3}$$

where H_i is the microhardness of the i-component (and/or phase) and φ_i is their weight fraction. Equation 3 is usually used for evaluation of the H of a blend or for characterization of some component (or phase) which are not accessible for direct determination of H. The additive law (Equation 3) has been frequently used for evaluation of the contribution of the crystalline, H_c, and amorphous, H_a, phases to the H of semicrystalline polymers [25] or for characterization of two-component, four-phase polymer blends [26].

3. Results

3.1. Microstructural characterization

Mechanical properties of multi-component systems, such as polymer blends and composites, depend primarily on the adhesion between the constituents [27]. In contrast to the blends of polyolefines, in dealing with blends of condensation polymers there are better opportunities for improving the adhesion on the phase boundary of the blend components, due to the possibility of chemical interactions [10, 11]. For this reason, in order to understand better the microhardness behaviour of MFC during their manufacture, an attempt was made to characterize morphologically the samples mainly with respect of the type and extent of interactions on the phase boundary between the blend components. For this purpose, previous X-ray measurements on the same samples [3] are complemented by observations of scanning electron microscopy (SEM). Furthermore, for the sake of comparison and mostly for more correct application of the additive law (Equation 3) to the blends, the neat components, the PET and PA6, were subjected to the same set of mechanical and thermal treatments as their blends during the manufacture of MFC.

Fig. 1 illustrates the WAXS patterns of the PET/PA6 blend subjected to different thermomechanical treatments. From these patterns, the following general conclusion can be drawn. For the starting zone-drawn sample (stage B-D, Fig. 1a) the appearance of the amorphous halo in the equator and the breadth of the crystalline reflections reveal a very good orientation of the chains along the axial direction and the presence of small and imperfect crystallites. After additional thermal treatment at 220 °C (stage B-D-1, Fig. 1b) the disappearance of the halo and the sharpening of the reflections in the equatorial and meridional directions evidence the improvement of chain orientation and perfection and/or growth of the crystallites.

Of particular interest is the blend annealed at 240 °C for 5 h (sample B-D-3) (Fig. 1c) where the scattering of the PA6 component appears in the form of Debye rings, showing the isotropy of that component. In addition, the orientation and perfection of the crystallites within the PET fraction is shown to remain unchanged. Prolonged annealing times (25 h) at the same temperature lead to the virtual disappearance of the PA6 Debye rings, as well as to an improvement of the crystallites perfection in the PET component (sample B-D-4, Fig. 1d).

These two processing steps of the blend are essential for the preparation of MFC. Short annealing at 240 °C, i.e. above the melting point of PA6, results in isotropization of this component forming in this way the matrix of the MFC. Actually, at this stage one converts the drawn bicomponent blend into a composite material. Longer annealing times (25 h) at 240 °C lead to the complete involvement of PA6 in a copolymer with the amorphous part of PET due to the chemical interaction of the two components. Obviously, the copolymers formed are characterized by random sequential order of repeating units, because no evidence for the crystallization of PA6 is available (Fig. 1d). This suggestion is supported by DSC measurements of the same samples where the melting peak of PA6 for the same sample (B-D-4) disappears completely [3]. DMTA [7] and IR [8] measurements also indicate the disappearance of the glass transition temperature, T_g, of PA6 for the same stage of treatment (B-D-4). Finally, the results of selective extraction of PA6 after the different stages of treatment as shown in Table II also lead to the same conclusion. One can see that any treatment not involving annealing at 240 °C allows the PA6 component (between 91% and 98%) to be almost completely removed from the blend. Short annealing times (5 h) at 240 °C allows extraction of roughly half of the PA6 amount, and extended (25 h) annealing, only 22% (Table II). These data illustrate, quite convincingly, the occurrence of chemical interactions between PET and PA6.

Table II summarizes some of the data for the coherence length of PET crystallites in various crystallographic directions, the X-ray long period and the crystallinity values derived from WAXS and DSC.

It is noteworthy that the two components, PET and PA6, behave rather differently with respect of their structure formation and crystallinity development. While neat PET shows almost constant crystallite sizes in (0 1 0) and ($\bar{1}$ 0 5) directions and, consequently, small changes in the X-ray crystallinity (~22–28%), neat PA6 shows a clear crystal size increase in the

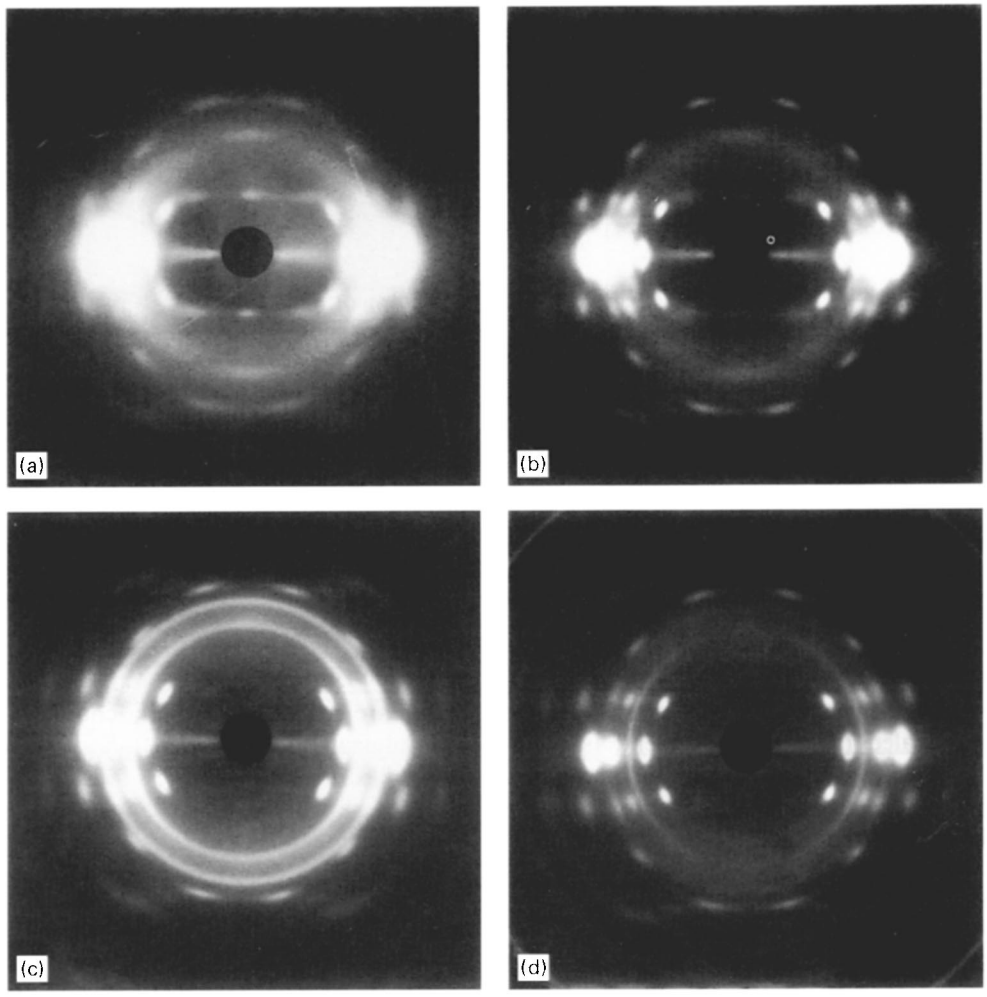

Figure 1 WAXS photographs of PET/PA6 blend, zone drawn and annealed at different temperatures corresponding to the various stages of MFC processing. (a) B-D, (b) B-D-1, (c) B-D-3, (d) B-D-4. For sample designation see Table I.

(2 0 0) direction (from 3.3 nm to 10.6 nm), although a rather small change in the w_c (WAXS) value (Table II). The long spacings, L, of the both polymers increase slightly with increase of T_a and t_a.

The value of w_c (DSC) increases for the neat PET steadily from 4% (for the starting undrawn, unannealed sample) up to 50% after annealing at 220 and 240 °C. The starting neat PA6 (sample PA-Q, Table I) shows a rather high initial crystallinity value (28%) which increases further up to 35% during the subsequent treatments (see Table II).

Quite interesting is the crystallinity development of the blend during processing as evaluated by the two techniques. WAXS only allows a determination of the total degree of crystallinity because of the overlapping of the respective scattering curves arising from PET and PA6. The total crystallinity value clearly decreases with increasing T_a and t_a from 46% to 27% (Table II). One can assume that this is related to the continuous involvement of PA6 in copolymers and thus to a decrease of its crystallization ability. This assumption is supported by the w_c data obtained by DSC.

Because the melting peaks of PET and PA6 are well separated in the DSC curves, it is possible to evaluate the contribution of each component to the formation of the total crystallinity as shown in Table II. In accordance with the behaviour of the neat homopolymers, one sees that the crystallinity of PET steadily increases from 17% up to 75%. Simultaneously the crystallinity of PA6 increases from 25% up to 36–38% after annealing of the blend at 220 °C. Thereafter the crystallinity of PA6 drops to 20% after annealing at 240 °C for 5 h (sample B-D-3, Table II). Prolonged annealing (25 h) at the same temperature results in a complete disappearance of PA6 crystallinity (sample B-D-4, Table II). This observation supports the above conclusions about chemical interaction between PA6 matrix and the amorphous part of the reinforcing oriented PET in the MFC.

3.2. Morphological observations

The improvement of adhesion between the matrix and the reinforcing microfibrils in MFC, as a result of transreactions between PET and PA6, is illustrated on the micrographs taken from blends after the various stages of preparation. The sample preparation for SEM observations was carried out in three different ways: (i) from the fracture surface after cooling in liquid nitrogen, (ii) from the fresh surface after peeling the sample, and (iii) after extraction with solvent selective for PA6 for to remove it from the blend. The results are displayed in Fig. 2. The first micrograph

TABLE II WAXS, SAXS and DSC parameters of zone-drawn and annealed neat PET, PA6 and PET/PA6 blend (1 : 1 by weight) [3] as well as weight loss after selective extraction of PA6 from the blend (referred to the PA6 content) [8]

	$D^{PET}_{(0\,1\,0)}$ (nm)	$D^{PET}_{(1\,0\,5)}$ (nm)	$D^{PA6}_{(2\,0\,0)}$ (nm)	L (nm)	w_c (WAXS)	w'_c (DSC)[a]		Weight loss (%)
PET-Q	–	–	–	–	–	0.04		–
PET-D	–	–	–	–	–	0.10		–
PET-D-1	8.6	5.0	–	11.8	0.22	0.44		–
PET-D-2	9.3	5.0	–	12.3	0.28	0.49		–
PET-D-4	8.8	5.2	–	13.0	0.21	0.48		–
PA-Q	–	–	3.3	–	–	0.28		–
PA-D	–	–	4.1	8.0	–	0.32		–
PA-D-1	–	–	9.7	10.4	0.22	0.35		–
PA-D-2	–	–	10.6	–	0.24	0.31		–
					(Total value)	PET	PA	
B-Q	–	–	–	–	–	0.17	0.25	98
B-D	–	–	3.7	–	–	0.39	0.29	96
B-D-1	7.5	4.8	8.3	12.0	0.46	0.46	0.38	91
B-D-2	7.8	4.8	8.6	11.8	0.47	0.48	0.36	80
B-D-3	8.2	5.1	12.2	12.8	0.28	0.53	0.19	62
B-D-4	7.8	5.0	–	–	0.27	0.75	–	22

[a] Corrected per gram of homopolymer in the blend.

(Fig. 2a) is taken from the fracture surface of the undrawn, unannealed (as-quenched) blend (sample B-Q, Table I). One can easily see the bicomponent character of the blend. It should be mentioned here that only for this investigation a different blend composition has been used 40/60 (by weight) in favour of PA6. This has been done in order to emphasize the particle character of the PET component. Rather uniform elliptical particles can be seen. Another important observation is the very smooth surface of the matrix in places from where the PET particles are peeled out. This is an indication of a very poor adhesion between both components of the blend.

Fig. 2b illustrates the presence of rather perfect PET fibrils after drawing and annealing the blend at 220 °C for 5 h (sample B-D-1, Table I). The fact that the fibrils have a quite perfect surface leads one to assume that no chemical interaction between matrix (PA6) and the reinforcing elements (PET) has taken place. This suggestion follows also from the observation that at this stage of treatment (B-D-1, Table I) the PA6 component can be removed by selective extraction almost completely (up to 91%, Table II).

Finally, on Fig. 2c one observes the fresh surface after peeling of the sample treated at 240 °C for 25 h (sample B-D-4, Table I). In this case, the rough surface indicates a good adhesion between microfibrils and matrix as result of transreactions between both blend components. The same conclusion can also be drawn from the result of selective extraction of PA6 – only 22% can be removed from the blend (sample B-I-4, Table II).

3.3. Microhardness characterization

Once the morphology of the blends and the level of adhesion between matrix and microfibrils were established, the microhardness characterization was performed. In a previous study [8] it was found that similarly to many polymer blends, the samples of MFC are coated by a thin (a couple of micrometres) skin of neat PET. In order to find out to what extent the measured microhardness reflects the behaviour of the blend and not just the behaviour of the outer skin, measurements with different loads were carried out for all the samples. The results are shown in Fig. 3 where the dependence between the load, P, and the indentation, d^2, is plotted. In all cases straight lines are observed. If, in the range of loads used, a change of the material quality occurred, one should then observe a variation in the slope of the straight lines of Fig. 3 as observed in other polymer blends [28].

Additional advantage of the measurements under various loads is the increased reliability of the data obtained. From the mutual disposition of the lines one can conclude qualitatively that the microhardness for all the samples increases with the progress of the processing, i.e. orientation and increase of temperature and annealing time. Quantitative information about the microhardness of the sample studied (Table I), derived from the curves in Fig. 3, is presented as histograms in Fig. 4.

In order to compare the experimental H values for the blends with the calculated ones the additive law (Equation 3) was applied in the following form

$$H = H^{PET}\varphi^{PET} + H^{PA}(1 - \varphi^{PET}) \quad (4)$$

where H^{PET} and H^{PA} are the experimentally measured values for the neat homopolymers and φ^{PET} and $(1 - \varphi^{PET})$ are their corresponding weight fractions. One can see from the histograms in Fig. 4 that the calculated values according to Equation 4 are close to the experimental values – the difference amounts to between 3% and 6%, except for the sample B-D-4, where it is only 0.6% (Fig. 4). Such good agreement between measured and calculated values in the last case could be related only to the extremely strong adhesion between matrix and reinforcing fibrils as demonstrated above. In this way the most favourable conditions for load transfer between matrix and microfibrils are ensured.

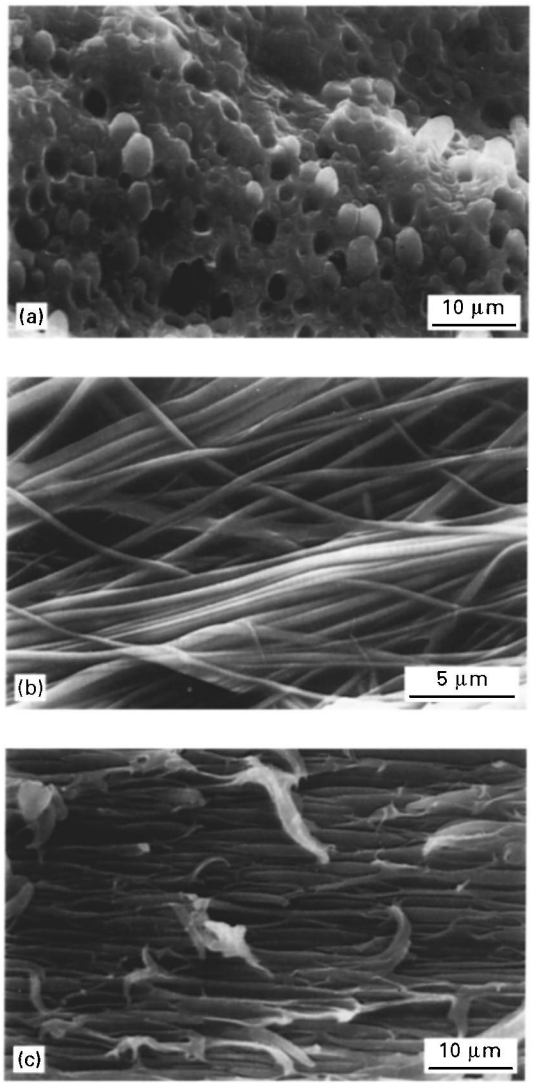

Figure 2 Scanning electron micrographs of PET/PA6 blend: (a) as-quenched (undrawn) (sample B-Q, Table I), taken from fracture surface after cooling in liquid nitrogen, (b) drawn and annealed at 220 °C for 5 h blend (sample B-D-1, Table I) after extraction of PA6 component by selective solvent; (c) sample B-D-4 after peeling of drawn and annealed at 240 °C for 25 h blend.

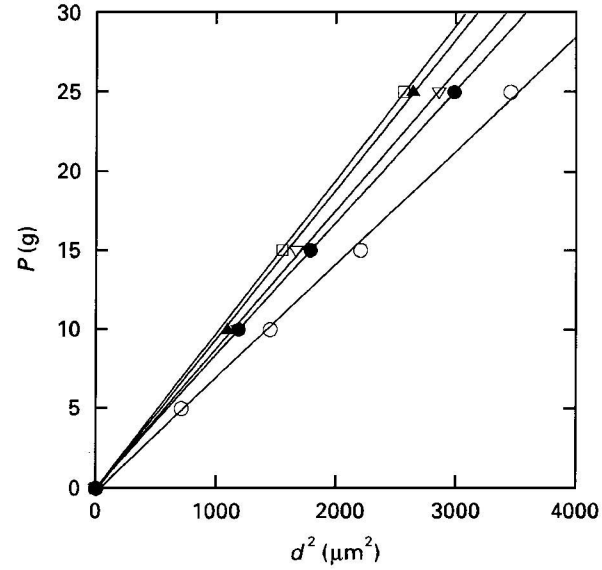

Figure 3 Plot of the load, P, against the square of the indentation diagonal, d^2, for PET/PA6 blend (1 : 1 by weight) corresponding to the respective processing stages according to Table I: (○) Q, (●) D, (▽) D-1, (▲) D-2, (□) D-4.

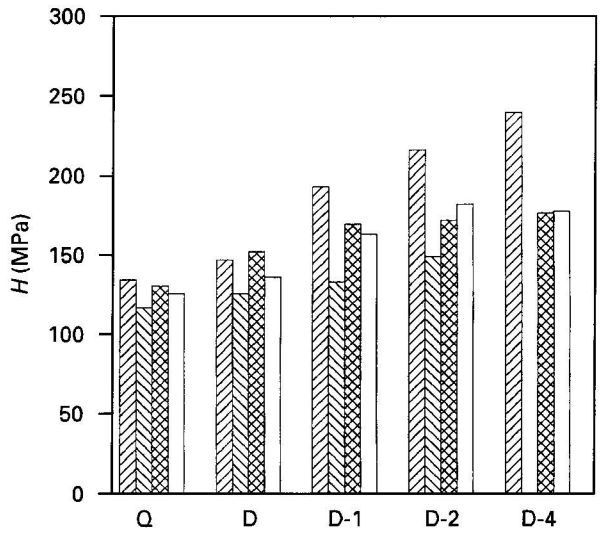

Figure 4 Microhardness of neat PET (first column of each processing stage), neat PA6 (second column) and their blend (1: 1 by weight) (third column) and the calculated H values (fourth column) after various mechanical and thermal treatments corresponding to the respective processing stages during manufacturing of MFC. The processing stages are designated in accordance with Table I.

4. Discussion

The fact that both the neat components and their blends are relatively well characterized with respect to their varying structure and morphology as a result of the applied mechanical and thermal treatments, permits the gradual variation of microhardness to be followed as a function of structural parameters. In this way one can obtain the H values for material components which are not accessible to direct experimental determination. Furthermore, having the extrapolated values for completely amorphous and fully crystalline homopolymers, and starting from the knowledge of the number of components (and/or phases), one can make use of the additive law (Equation 3) for evaluation of the mechanical properties of components which cannot be isolated or do not exist as individual material. A good example of this are the PET microfibrils which represent one of the targets of this study.

4.1. Influence of crystal size and crystallinity on hardness

Let us come back to Table II where the structural and morphological characteristics of the samples studied are summarized. It should be noted that the observed disagreement between w_c values gained from WAXS and DSC techniques is only apparent. First of all, it is well known that the numerical values of w_c for a same set of samples depend on the technique used [29]. The conclusion that w_c (WAXS) values do not change in contrast to the w_c (DSC) is also misleading, because for the same set of treatment conditions both techniques lead to rather constant values (Table II). This is because these treatment conditions (T_a of 220 and

240 °C, and t_a of 5 and 25 h) favour the crystallization and almost maximum crystallinity values for the two neat homopolymers is achieved (Table II).

Fig. 5 shows the dependence of H versus w_c (DSC) for the two neat homopolymers. It is seen that H increases linearly with w_c for both PET and PA6. Interesting enough, the two straight lines are not far from being parallel to each other suggesting that the crystallinity increase contributes nearly in the same way to the development of the microhardness in the two cases.

The extrapolation of the straight lines allows one to obtain the H values for the completely amorphous ($H_a^{PET} \sim 128$ MPA; $H_a^{PA} \sim 52$ MPa) and completely crystalline ($H_c^{PET} \sim 294$ MPA; $H_c^{PA} \sim 283$ MPa) polymers, which for the PA6 is of particular importance because it is not accessible in the fully amorphous state for such measurements. This is the first evaluation of the microhardness of a fully amorphous polyamide.

The crystal structure of PA6 is distinguished by another peculiarity. In contrast to PET it shows practically the same degree of crystallinity (around 30%) regardless of the treatment conditions but unlike PET shows a clear increase in the crystal size (Table II). These two facts offer a good possibility for evaluation of the crystal size contribution to the microhardness of the polyamide. The dependence of H against $1/D_{200}$ for PA6 is plotted in Fig. 6. The extrapolation of the straight line yields for $1/D_{200} = 0$ the H value of PA6 (composed by 70% amorphous phase and roughly 30% crystalline phase) for infinitely large crystals. The H value obtained amounts to 153 MPa. This means that a completely crystalline PA6 comprising infinitely large crystals should have a microhardness value of about $H^{\infty} = 460$ MPa. It is important to note that the previous extrapolations of Fig. 5 also give the H values of completely crystalline species but for polymer comprising crystallites with finite sizes and not infinitely large ones. For this reason, the H^{∞} value of

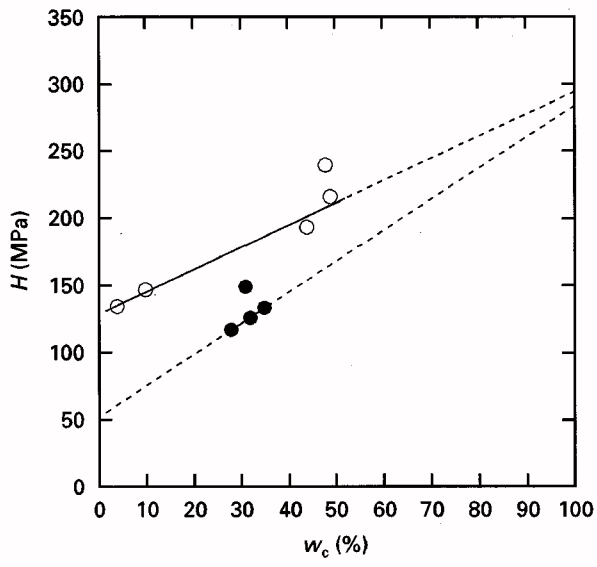

Figure 5 Variation of microhardness of (○) neat PET and (●) PA6 with increasing degree of crystallinity w_c (DSC) developed during the mechanical and thermal treatments corresponding to the various stages of MFC formation.

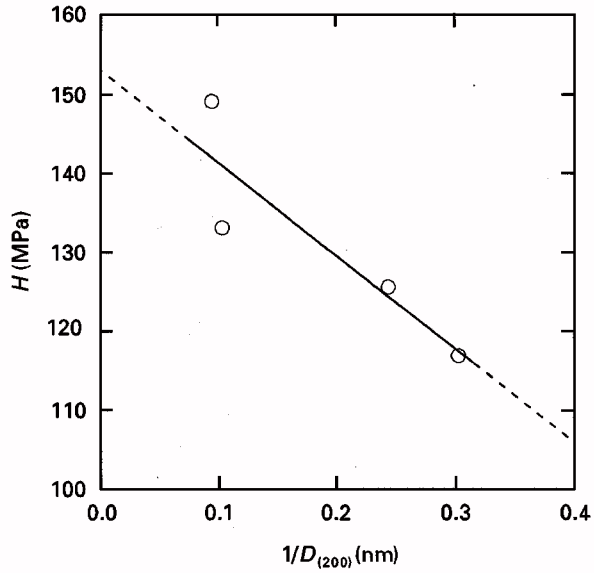

Figure 6 Plot of H versus $1/D_{(200)}$ for samples with the same crystallinity of neat PA6 subject to mechanical and thermal treatments corresponding to the various stages of MFC formation.

460 MPa can be considered as an ideal (equilibrium) microhardness of PA6, similarly to the ideal melting temperature.

Before using the H_a and H_c extrapolated values for further calculation, let us comment on the, at first glance, unexpected microhardness behaviour for the neat homopolymers annealed at the highest temperatures, which is distinguished by almost constant w_c values regardless of the T_a and t_a (Table II).

From Fig. 5 one can see that for each homopolymer two samples exist distinguished by constant w_c (DSC) values (Table II, samples PET-D-2 and PET-D-4, samples PA-D and PA-D-2) but differing in their H values, one of them disobeying the linear relationship between H and w_c. What can be the reason for such a behaviour? From Table II one can conclude that such a sharp rise in H cannot originate from an increase either in crystallinity or in crystal size, as usually interpreted [25]. Both parameters have practically the same values for the two samples of each neat homopolymer (Table II). To explain this peculiarity in the H behaviour one may suggest that prolonged annealing (25 h) at constant relatively high temperatures close to the melting (T_a for PA6 220 °C and for PET 240 °C, Table I) causes a perfectioning of crystalline phase and not necessarily an increase in the degree of crystallinity or crystal size. As demonstrated earlier for drawn PET [30] the perfectioning during extended annealing consists of continuous removal of defects from the crystallites into the amorphous phase. This process will result in some increase in the long spacing, L, at cost of the amorphous phase; but not in a crystal thickening as usually interpreted for polymers with rather homogeneous chain structure. It is well known that PET, strictly speaking, is always a copolymer, the third monomer being the diethylene glycol ether (DEG). Model studies on PET with various DEG-content support this mechanism of perfectioning [31, 32].

The observed slight increase (about 10%) in the L-values for constant crystallite size, particularly for PET (Table II) is also in favour of such interpretation. Thus, one can conclude that the observed increase in H can be related to the occurrence of more perfect and consequently "harder" crystals of the same size.

4.2. Hardness of MFC: additivity behaviour

As mentioned above, the application of the additive law (Equation 3) supposes the knowledge of a number of the components (or phases) with given values of their microhardness and weight fractions. What is not explicitly said in this equation is the type and the extent of mutual dispersion of the components as well as the quality of the adhesion on the contact surface boundary between the components (phases). We wish to stress here that this aspect has an influence on the reliability of the H values derived from the additive law.

In the present study, we deal with well characterized samples with respect to the number of components and phases. The neat homopolymers consist of one component comprising two phases. Their blends are two-components with four different phases. Depending on the treatment conditions the number of components and/or of phases can be reduced. Our conclusion that during annealing of the blends at 240 °C for longer time intensive chemical interactions take place, is in accordance with many results on similar systems – blends of condensation polymers. In fact, exchange reactions between adjacent functional groups, generating *in situ* copolymers, are reported to be a possible method for compatibilizing condensation polymers [1, 33–43]. It should be noted that exchange reactions proceed considerably faster in the molten state. The addition of an appropriate catalyst still further increases the conversion rate. Thus, for instance, Kamal *et al.* [35] report 5%–23% conversion of the ester–amide interchange reaction in a PET/PA-66 blend during a single pass (2–4 min) in an extruder at 300–310 °C, catalysed with 0.2% *p*-toluenesulphonic acid. Andresen and Zachmann [33] report full conversion of transesterification in a PET/poly(ethylene–2,6-napthalene dicarboxylate) blend during melt-pressing for 10 min at 280 °C. Gattiglia *et al.* [37] have observed the formation of block copolymers after melt mixing a 75/25 by weight PA6/PC blend at 240 °C for 45 min. Formation of segmented copolyamides due to transamidation has been observed during melt mixing of PA6 and poly (*m*-xylene adipamide) [38] as well as PA-46 and PA6 [39]. Hours are required for the occurrence of such reactions in the solid state. Solid-state reactions in linear polycondensates are particularly favoured at high annealing temperatures and occur in the non-crystalline phases, which enjoy relatively higher chain mobility than the crystalline phase [11].

For this reason the PET/PA6 blends treated at temperatures below 240 °C should be a two-component and four-phase system as can be concluded also from the WAXS (Fig. 1). After annealing at 240 °C, especially for 25 h (sample B-D-4) the system converts itself into a two-component one (matrix and reinforcing microfibrils) being three or possibly two-phase systems (amorphous matrix comprising 25% of the total amount of PET and almost fully crystalline one-phase microfibrils). Starting from these considerations and making use of the extrapolated data for the H_a and H_c values of the two homopolymers (Fig. 6) the additive law (Equation 3) was used in the respective form in order to derive the H values for the blends and the MFC and compare them with the experimentally measured ones. Only after such a verification of the additive law (Equation 7) can the evaluation of the microhardness of the PET microfibrils be carried out.

Using the parallel model for PET we may write

$$H^{PET} = H_c^{PET} w_c^{PET} + H_a^{PET}(1 - w_c^{PET}) \quad (5)$$

For PA we may write

$$H^{PA} = H_c^{PA} w_c^{PA} + H_a^{PA}(1 - w_c^{PA}) \quad (6)$$

By combination of Equations 4, 5 and 6 the hardness for the two-component and four-phase system can be rewritten in the following form

$$H = \phi^{PET}[H_a^{PET}(1 - w_c^{PET}) + H_c^{PET} w_c^{PET}] + (1 - \phi^{PET})[H_a^{PA}(1 - w_c^{PA}) + H_c^{PA} w_c^{PA}] \quad (7)$$

Applying the w_c (DSC) data from Table II for the weight fraction of each phase, the values derived for the microhardness, H, of the blends by means of Equation 7 are given in Table III. The comparison shows a good agreement between both sets of values. The only striking deviation is for the sample B-D-4 for which the calculated H value according to the Equation 7 is much lower. Such a result means that the assumed H_c^{PET} values assigned in this particular case to the PET microfibrils are too low. In accordance with above consideration about the morphology of this sample, one has to modify Equation 7 accordingly, taking into account that for the sample B-D-4 the crystallinity $w_c^{PA} = 0$ (see Fig. 1, Table II). Because, in the blend PET/PA6 = 1 : 1 (by weight) $\phi = 0.5$, the additive law for estimation of the H of PET microfibrils (Equation 7) should be presented in the following form

$$H = 0.5(w_a^{PA} H_a^{PA} + w_a^{PET} H_a^{PET} + w_c^{PET} H_c^{PET}) \quad (8)$$

The first two members refer to the matrix of MFC which is just one single component amorphous phase.

The above expression for the microhardness of the amorphous matrix of the MFC (Fig. 1, Table II, Sample B-D-4) is acceptable, because it was demonstrated [19] that the H values for completely amorphous copolymers (with random sequential order) obey the additive law provided the H_a values for the respective homopolymers are used.

In this way one obtains for the microhardness of the microfibrils, H_c^{PET}, a value of 360 MPa. This value is higher than any other reported for PET crystallized in a common way, and approaches the measured value for PET crystallized under high pressure, the latter being 400 MPa [44].

TABLE III Mechanical properties of zone-drawn and annealed neat PET, PA6 and PET/PA6 blend (1:1 weight)

Sample	Young's modulus, E (GPa)	Tensile strength, σ (MPa)	Elongation at break, ε (%)	Microhardness	
				H^{exp}	H^{cal} Equation 7
PET-Q	1.1	55	320	134	135
PET-D	9.4	221	9	147	145
PET-D-1	10.6	288	17	194	203
PET-D-2	11.4	316	14	216	209
PET-D-4	9.5	208	28	240	208
PA-Q	0.2	55	90	117	117
PA-D	4.5	342	31	126	126
PA-D-1	4.8	312	36	133	133
PA-D-2	2.7	99	56	150	140
B-Q	–	–	–	131	134
B-D	8.8	330	36	152	156
B-D-1	9.3	346	31	170	172
B-D-2	9.8	286	29	172	172
B-D-3	7.8	159	150	175[a]	156
B-D-4	8.6	180	21	177	152

[a] This value is obtained by averaging the neighbouring two (samples B-D-2 and B-D-4).

The obtained H value for PET microfibrils is supported also by similar calculations with the sample B-D-3. By means of the experimental H value for this sample and applying Equation 7, an H_c^{PET}-value of 365 MPa is again obtained. These results explain the large difference between "measured" and calculated H values of this sample (Table III, sample B-D-3) when for the H_c^{PET} (in the present case this is the hardness of PET microfibrils) the extrapolated value, $H_c^{PET} = 294$ MPa, is adopted.

This surprisingly high H value for the reinforcing PET microfibrils can be explained by taking into account the peculiarities in the structure of the MFC. It is useful in this respect to recall the conclusions concerning the crystalline structure and morphology of microfibrils derived from a previous study of the same system subjected to the same mechanical and thermal treatments [3].

Zone drawing results in a high orientation of chains and crystallites. Subsequent annealing at 220 °C results in crystallite growth, an ordered stacking of crystalline lamellae and an increased degree of crystallinity. Direct transmission electron microscopy [45–53] (including work on PET, one of the homopolymers used here [51–53]) has shown that the crystallization of oriented systems begins typically with the formation of fine microfibrillar precursor crystallites with the fibrils parallel to the fibril axis. As a next stage, these systems transform into stacks of lamellar crystals, the stacking axis being parallel to the original fibrous crystallites and the chain axis still lying along the original fibril axis [53, 54]. The stacks can be relatively long in the stacking direction and narrow transverse to it. One can thus think of such an entity as a microfibril [53].

The microfibrils should be almost completely crystalline as can be concluded from the following consideration. The measured values w_c (DSC) of 75% refer to the total amount of PET in the blend. The amorphous part (25%) of PET has been involved in copolymers with PA6 as indicated above, which is not the case with the crystalline PET (microfibrils). For this reason and because of the outlined structure formation peculiarities, the microfibrils should be of very high crystallinity. This explanation is supported also by another observation. As mentioned above PET crystallized under pressure shows a value of $H = 400$ MPa [44]. Detailed structure analysis of such samples showed that they are almost completely crystalline ($w_c = 90\%$) and consist of rather large crystals (crystal sizes around 10–15 nm [44]). Only by this similarity in the structure characteristics can one obtain extremely high H values.

In the present case, isotropization due to melting of the PA6 component is established at $T_a = 240$ °C, the fibrillized PET preserving, however, its orientation and microfibrillar structure. As a result, a composite-like material is obtained, comprising an isotropic semicrystalline (sample B-D-3) or non-crystalline (sample B-D-4) matrix of PA6 reinforced with almost fully crystalline, microfibrillized PET (Figs 1 and 2, Table II).

4.3. Macroscopic mechanical properties

The important role of the PET component is seen in Table III, where some macroscopic mechanical properties of the blends are reported. The blend specimens with composite-like structure (samples B-D-3 and B-D-4) show elastic moduli of 7.8 and 8.6 GPa, respectively, and tensile strengths of 159 and 180 MPa, respectively. These values are almost identical to the modulus ($E \approx 7$–8 GPa) and strength ($\sigma \approx 150$–160 MPa) values observed for glass fibre-reinforced (25%–40% glass fibres) engineering plastic nylon 66, and are five to six times higher than those of semicrystalline isotropic polyamides ($E \approx 1$–1.5 GPa and $\sigma \approx 40$–50 MPa) [54]. It is convenient to note that the measured modulus of these blend samples is greater than that predicted for parallel loading of the two components. Because parallel loading produces an upper bound on the modulus, it appears that blending

with PA6 induces a new microstructural state for the PET component, perhaps microfibrils with a higher aspect ratio.

The still higher values of E and σ of the blend annealed at 220 °C (samples B-D-1 and B-D-2, Table III) are noteworthy. It is possible that this behaviour is due to the presence of a higher number of intra- and interfibrillar tie molecules under stress in these samples, as compared to those annealed at 240 °C.

5. Conclusions

1. Annealing of the drawn PET/PA6 blend at 240 °C (i.e. between the T_m values of the neat components) results in the formation of composites with a PA6 dominant amorphous matrix reinforced by the preserved PET microfibrils. The microhardness of amorphous PA6 has been evaluated for the first time ($H_a^{PA} = 52$ Pa). In addition, the transreactions between the PET and PA6 lead to an improvement of the adhesion between matrix and microfibrils resulting in high microhardness values.

2. The additivity law is applied for microhardness characterization of the fundamental element of microfibrilar-reinforced composites: the microfibrils which are not accessible for direct measurements. The surprisingly high value of 360 MPa obtained is explained by the peculiar structure of these morphological elements: high orientation and large crystallinity values.

3. Extrapolation of H versus reciprocal crystal size values ($1/D$) for neat PA6 samples having the same crystallinity leads to an H value for infinite large crystals $H^{\infty} = 460$ MPa.

4. The importance of the knowledge about the type and extent of the mutual dispersion of the components, as well, as the adhesion between them is emphasized for the proper application of the additive law in microhardness studies.

Acknowledgements

The authors are grateful to DGICYT, Spain (Grant PB94-0049) for the support of this investigation. The partial support of DFG, Germany (Grant DFG-FR 675/21-1) is also acknowledged. One of us (S.F.) deeply appreciates the tenure of a sabbatical grant from DGICYT, Spain.

References

1. L. A. UTRACKI, "Polymer Alloys and Blends" (Hanser, Munich, 1989).
2. M. EVSTATIEV and S. FAKIROV, *Polymer* **33** (1992) 877.
3. S. FAKIROV, M. EVSTATIEV and J. M. SCHULTZ, *ibid.* **34** (1993) 4669.
4. *Idem, Macromolecules* **26** (1993) 5219.
5. S. FAKIROV and M. EVSTATIEV, *Adv. Mater.* **6** (1994) 395.
6. M. EVSTATIEV, S. FAKIROV and K. FRIEDRICH, *Appl. Compos. Mater.* **2** (1995) 93.
7. T. SERHATKULU, B. ERMAN, I. BAHAR, S. FAKIROV, M. EVSTATIEV and D. SAPUDJIEVA, *Polymer* **36** (1995) 2371.
8. M. EVSTATIEV, N. NIKOLOV and S. FAKIROV, *ibid.* **37** (1996) 4455.
9. M. EVSTATIEV, J. M. SCHULTZ, S. PETROVICH and S. FAKIROV, *Polymer*, submitted.
10. P. J. FLORY, "Principles of Polymer Chemistry" (Cornell University Press, Ithaca, NY, 1953).
11. S. FAKIROV, in "Solid State Behavior in Linear Polyesters and Polyamides", edited by J. M. Schultz and S. Fakirov (Prentice Hall, Englewood Cliffs, NJ, 1990) p. 1.
12. M. FISCHER, in "The Interfacial Interactions in Polymeric Composites", edited by G. Akovali (Kluwer, Dordrecht, 1992) p 415.
13. R. HOLSTI-MIETTINEN, J. SEPPAELAE and O. T. IKKALA, *Polym. Engng Sci.* **32** (1992) 868.
14. A. R. PADWA, *ibid.* **32** (1992) 1703.
15. F. J. BALTA CALLEJA, C. SANTA CRUZ, C. SAWATARI and T. ASANO, *Macromolecules* **23** (1990) 5352.
16. J. MARTINEZ-SALAZAR and F. J. BALTA CALLEJA, *J. Mater. Sci. Lett.* **4** (1985) 324.
17. T. A. EZQUERRA, F. J. BALTA CALLEJA, L. GIRI and Z. ROSLANIEC, *J. Macromol. Sci. Phys.*, **B36** (1997) 335.
18. F. ANIA, J. MARTINEZ-SALAZAR and F. J. BALTA CALLEJA, *J. Mater. Sci.* **24** (1989) 2934.
19. F. J. BALTA CALLEJA, L. GIRI, T. A. EZQUERRA, S. FAKIROV and Z. ROSLANIEC, *J. Macromol. Sci. Phys.*, **B36** (1997) 655.
20. T. KUNUGI, C. ICHJINOSE and A. SUZUKI, *J. Appl. Polym. Sci.* **31** (1981) 429.
21. T. KUNUGI, I. AKIYAMA and M. HASHIMOTO, *Polymer* **23** (1982) 1199.
22. S. GOGOLEWSKI, and A. J. PENNINGS, *ibid.* **18** (1977) 654.
23. B. WUNDERLICH, *Polym. Engng Sci.* **18** (1979) 431.
24. F. J. BALTA CALLEJA and C. G. VONK, "X-ray Scattering of Synthetic Polymers" (Elsevier, Amsterdam, 1989) p. 129.
25. F. J. BALTA CALLEJA, *Adv. Polym. Sci.* **66** (1985) 117.
26. C. SANTA CRUZ, F. J. BALTA CALLEJA, H. G. ZACHMANN and D. CHEN, *J. Mater. Sci.* **27** (1992) 2161.
27. D. HULL, "An Introduction to Composite Materials" (Cambridge University Press, Cambridge, 1987).
28. F. J. BALTA CALLEJA, D. R. RUEDA, J. M. AYRES DE CAMPOS and M. E. CAGIAO, *J. Mater. Sci.* **23** (1988) 4487.
29. S. FAKIROV, "Structure and Properties of Polymers" (Sofia Press, Sofia, 1985) (distributed by Martin-Nijhoff, Holland).
30. E. W. FISCHER and S. FAKIROV, *J. Mater. Sci.* **11** (1976) 1041.
31. S. FAKIROV, *Polymer* **21** (1980) 373.
32. S. FAKIROV, I. SEGANOV and L. PRANGOVA, *Makromol. Chem.* **184** (1984) 807.
33. E. ANDRESEN and H. G. ZACHMANN, *Coll. Polym. Sci.* **272** (1994) 1352.
34. M. KIMURA and R. S. PORTER, *J. Polym. Sci. Polym. Phys. Ed.* **21** (1983) 267.
35. M. R. KAMAL, M. A. SAHTO and L. A. UTRACKI, *Polym. Engng Sci.* **22** (1982) 1127.
36. J. DEVAUX, P. GODARD and J. P. MERCIER, *ibid.* **22** (1982) 229.
37. E. GATTIGLIA, F. P. LA MANTIA, A. TARTURRO and A. VALENZA, *Polym. Bull.* **21** (1989) 47.
38. Y. TAKEDA and D. R. PAUL, *Polymer* **32** (1991) 2171.
39. K. L. L. EERSELS and G. GROENINCKX, *ibid.* **37** (1996) 983.
40. D. ROGER MOORE and L. J. MATHIAS, *J. Appl. Polym. Sci.* **32** (1986) 6299.
41. T. S. ELLIS, *Polymer* **33** (1992) 1469.
42. *Idem, Macromolecules* **22** (1989) 712.
43. A. VERMA, B. L. DEOPURA and A. K. SENGUPTA, *J. Appl. Polym. Sci.* **31** (1986) 747.
44. N. STRIBECK, H. G. ZACHMANN, R. K. BAYER and F. J. BALTA CALLEJA, *J. Mater. Sci.* **32** (1997) 1639.
45. J. PETERMANN and R. M. GOHIL, *J. Mater. Sci.* **14** (1979) 2260.
46. *Idem, J. Polym. Sci. Polym. Lett. Edn* **18** (1980) 781.
47. J. PETERMANN, *Makromol. Chem.* **182** (1981) 613.
48. J. PETERMANN, R. M. GOHIL, J. M. SCHULTZ, R. W. HENDRICKS and J. S. LIN, *J. Mater. Sci.* **16** (1981) 265.

49. J. RAU, R. M. GOHIL, J. PETERMANN and J. M. SCHULTZ, *Coll. Polym. Sci.* **259** (1981) 241.
50. R. MURRAY, H. A. DAVIS and P. TUCKER, *J. Appl. Polym. Sci. Appl. Polym. Symp.* **33** (1978) 177.
51. J. PETERMANN and U. RIECK, *J. Mater. Sci.* **22** (1987) 1120.
52. H. CHANG, J. M. SCHULTZ and R. M. GOHIL, *J. Macromol. Sci. Phys.* **B32** (1993) 99.
53. J. M. SCHULTZ and J. PETERMANN, *Coll. Polym. Sci.* **262** (1984) 294.
54. DuPont de Nemours International SA, Switzerland, Brochure E-52863 (1986).

Received 15 April 1997
and accepted 3 March 1998